Deep Learning-based Prediction of Atrial Local Fibrosis from In Silico Intracavitary Electrograms

Santiago Moreno-Pineda, Giada S. Romitti, Duna De Luis-Moura, María Termenón-Rivas, Alejandro Liberos, Miguel Rodrigo

CoMMLab, Universitat de València, València, Spain

Abstract

Atrial fibrillation (AF) is driven by structural remodeling, such as interstitial fibrosis, although its detection in clinical set-ups remain unsolved. This study develops a computational tool to identify fibrotic substrate from intracardiac electrograms (EGMs).

Using a virtual cohort of N=19 bi-atrial anatomies, we extracted unipolar and bipolar EGM activation windows from simulated healthy and fibrotic tissue during AF. We optimized a 1D-CNN to predict fibrosis infiltration from EGM traces, and compared the performance of signal type, electrode-to-tissue distance, and spatial labeling radius.

Results showed bipolar EGMs, with 0.2 mm recording distances, and 3 mm labeling radii optimized fibrosis detection. On test set, the 1D-CNN achieved a window-level AUPR of 0.94 and an EGM-level Dice of 0.87. Mapped onto 3D geometries, predictions accurately delineated complex fibrotic patches without generating excessive false positives.

1D-CNN architectures can effectively extract information of the atrial substrate from simulated EGMs to accurately predict atrial fibrosis. Clinically, this computational pipeline could provide an accessible, real-time tool to optimize therapeutic planning and personalize AF ablation strategies.

1. Introduction

Atrial fibrillation (AF) remains the most prevalent sustained cardiac arrhythmia with a prevalence that has increased markedly over the last two decades [1]. AF is intimately linked to the structural and functional remodeling of the atrial myocardium, with interstitial fibrosis acting as a primary arrhythmogenic driver. Fibrotic tissue disrupts normal electrical propagation facilitating the formation of reentrant wavelets that sustain AF [2]. Accurately mapping this fibrotic substrate is crucial for patient stratification and for guiding personalized ablation strategies to improve long-term outcomes.

While late gadolinium magnetic resonance imaging (LGE-MRI) remains the non-invasive gold standard for mapping atrial fibrosis, lack of standardization, poor reproducibility, and high costs hinder its clinical application. In contrast, intracardiac electrograms (EGMs) provide an accessible, real-time alternative. Due to visual EGM inspection and classification is highly subjective, advanced computational tools are essential. Recent solutions include machine learning algorithms to detect fibrosis via signal complexity [2], omnipolar mapping [3], and the eigenvalue dominance ratio, which evaluates unipolar dispersion for robust fibrosis detection despite noise and variable electrode contact [4].

In this context, we propose a customized one-dimensional convolutional neural network (1D-CNN) to automatically identify fibrotic substrate directly from raw EGMs, eliminating the need for prior feature extraction. Using a virtual bi-atrial cohort, we systematically evaluated data configurations regarding signal type, electrode-to-endocardium distance, and spatial labeling resolution. Ultimately, this computational tool aims to accurately characterize atrial substrate, optimizing therapeutic planning and guiding personalized ablation strategies.

2. Materials and methods

2.1. Intracavitary electrograms during atrial fibrillation

Atrial electrophysiology was simulated using the Koivumäki et al. human cell model [5] and a monodomain formulation on tetrahedral meshes, accounting for fiber orientation and anisotropy [6]. A GPU-based solver [7] computed electrical propagation with a 20 μs time step. We employed N=19 bi-atrial anatomies derived via Statistical Shape Modeling [6], specifically selected for their high AF vulnerability, defined by arrhythmia inducibility across seven pacing sites. These models incorporated 3.88% to 25.98% fibrosis infiltration based on the Utah classification. Following our previous work [8], fibrotic

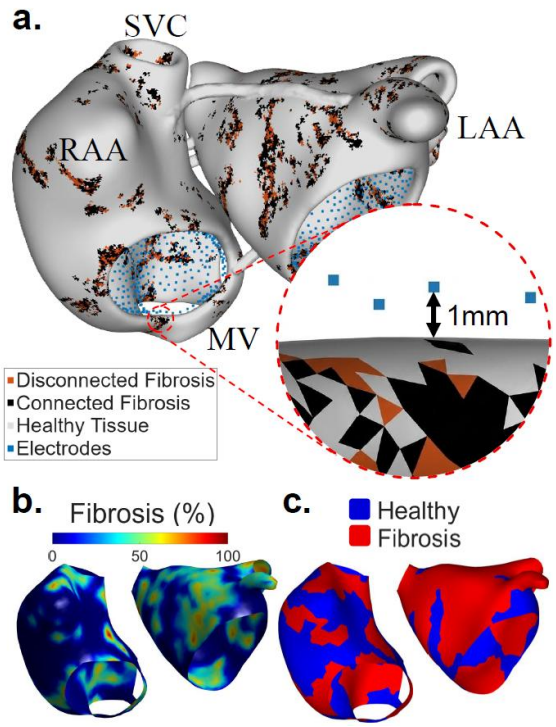

Figure 1. a) Bi-atrial model showing different types of tissue and the electrode grid b) ground-truth and c) binary fibrotic maps.

modeling (Fig. 1a) included disconnected nodes (zero conductivity) and connected nodes (specific ionic remodeling), alongside varied global electrical remodeling parameters to represent diverse pathological conditions.

Intracavitary EGMs were computed from simulated action potentials using a grid of virtual electrodes, defined as a shell, created by offsetting the endocardial surface by 1 and 0.2 mm and remeshing it with a 2 mm inter-node distance (Fig. 1a). Following our previous mathematical formulation [9], unipolar signals were calculated from the spatial gradient of the transmembrane potential relative to each electrode. Bipolar EGMs were subsequently derived by calculating the potential difference between each virtual electrode and its nearest neighbor within a 1 to 3 mm inter-electrode distance. a shows the distinct morphological signatures of the EGMs from both healthy and fibrotic tissue.

2.3. Dataset construction

To prevent temporal bias, we extracted isolated 200 ms EGM windows of local activations exclusively during sustained AF (b). Local activation times (LATs) were identified using the first derivative of the EGMs ($min(dV/dt)$) for unipolar signals, whereas for bipolar signals, were assigned to the maximum absolute value of the signal ($max|V|$). Once detected, each window was symmetrically segmented using a fixed duration of 100 ms

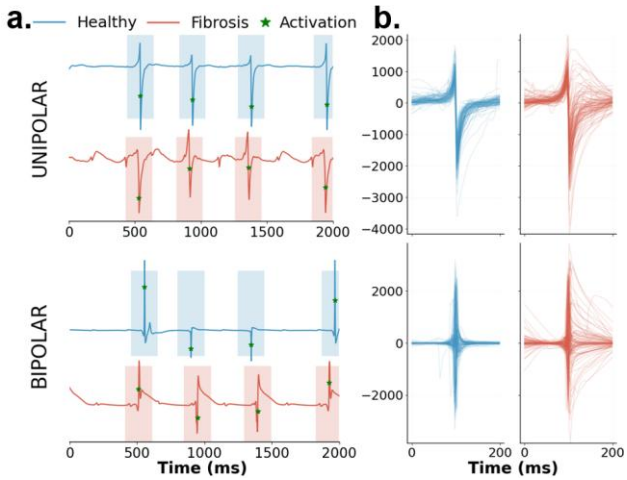

Figure 2. (a) unipolar and bipolar EGMs, highlighting morphological differences between healthy (blue) and fibrotic (red) tissue; and (b) extracted windows.

before and after the activation instant. Importantly, no amplitude normalization was applied to the extracted windows in order to preserve amplitude variability of EGMs, which is a key biomarker highly correlated with the presence of underlying fibrotic substrate.

The ground-truth for each EGM was generated by computing the proportion of fibrotic nodes within a specific spherical radius R surrounding the virtual electrode. Four different radii were evaluated (R ∈ {3, 5, 8, 10} mm), from which we obtained continuous fibrotic maps (see b) for each virtual anatomy. For network training, these fibrotic maps were binarized (c). Thresholds for binarization were dynamically defined using the median value of each label's distribution, computed from the entire dataset, ranging from 2.46 to 13.9 % of fibrosis.

Finally, to ensure robust evaluation and prevent data leakage, the datasets were partitioned using a patient-level stratification strategy. The virtual cohort was divided into 10 models for training, 5 for validation, and 4 for testing. Table 1 summarizes the number of signals across the different data partitions for both unipolar and bipolar EGMs.

Table 1. Distribution of generated EGMs across data partitions, electrode-to-endocardium distances (shell distance).

Data Partition	Shell Distance	No. of Unipolar EGMs	No. of Bipolar EGMs
Train (N=10)	1 mm	36,082	101,332
	0.2 mm	47,919	175,512
Validation (N=5)	1 mm	18,844	53,006
	0.2 mm	23,912	85,378
Test (N=4)	1 mm	13,444	37,552
	0.2 mm	18,178	66,325

2.4. Model architecture and training

The proposed architecture processes single-channel isolated EGM windows, extracting features via two sequential convolutional blocks (64 and 32 filters) that integrate 1D convolution, batch normalization, ReLU activation, max-pooling, and dropout regularization. The resulting feature maps are then flattened and fed into a fully connected classifier with a 128-neuron hidden layer, which projects to a single output neuron for the binary classification of the fibrotic substrate.

To assess data configuration, a baseline model (kernel size 16, pool size 8, dropout 0.3, learning rate 1e-4, 60 epochs) evaluated the impact of signal type, electrode-to-endocardium distance, and labeling radius. Performance was primarily assessed using the Area Under the Precision-Recall Curve (AUPR), alongside Precision, Recall, and F1-score. Following the identification of the optimal data configuration, a comprehensive grid search was conducted to fine-tune the convolutional kernel and pooling sizes, dropout probabilities, and learning rates, in order to maximizing the model's predictive capabilities.

3. Results

In the initial data configuration analysis, we observed that bipolar electrograms demonstrated superior performance over unipolar signals. As can be seen in the left panel of , the bipolar configuration achieved a notably higher median AUPR and a higher overall distribution of scores, indicating a stronger capacity to capture local electrophysiological features associated with fibrosis.

The evaluation of the electrode-to-endocardium distance revealed a preference for closer proximity. The 0.2 mm shell distance yielded a higher median AUPR compared to 1 mm, suggesting that minimizing the gap between the virtual electrode and the tissue maximizes the fidelity of the extracted intracavitary features. These findings are consistent with the results presented in [2], where electrode-to-tissue distances close to zero millimeters showed higher accuracy in fibrosis prediction.

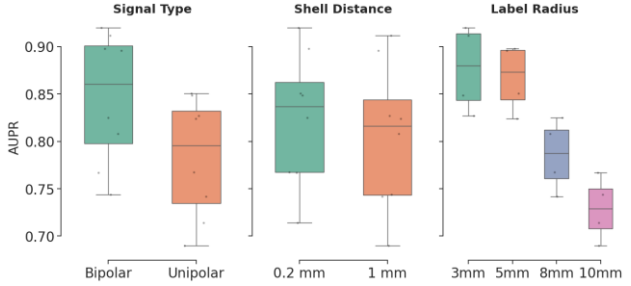

Figure 3. Boxplots illustrate the impact of signal type (left), virtual electrode-to-endocardium distance (middle), and ground-truth labeling radius (right) on the predictive performance of the baseline model.

Moreover, the analysis of the ground-truth labeling radius demonstrated a strong negative correlation with model performance. The highest AUPR scores were concentrated at smaller, highly localized radii (3 mm and 5 mm), with performance progressively decreasing as the radius reached 10 mm. This trend was expected and is consistent with the EGM generation algorithm, which penalizes the contribution of remote nodes from the atrial mesh compared to closer ones [9].

After selecting the optimal data configuration (bipolar electrograms, 0.2 mm shell distance, and R = 3 mm), we performed a systematic grid search to identify the hyperparameters that best capture the high-frequency components (fractionation) and attenuated amplitudes characteristic of EGMs recorded in fibrotic regions. The evaluation revealed that the network demonstrated high overall robustness in validation AUPR (0.923 ± 0.007; 95% CI: [0.921, 0.924]) across the 81 tested configurations. Despite this general stability, the results showed that the model works better with lower downsampling factors. Specifically, a small pooling size (2) and a low dropout rate (0.1) were necessary to avoid over-compressing the signal and losing important details. Finally, using a larger kernel size (16) allowed the network to look at a wider window of the signal, helping it to better recognize the morphology of local activations.

To assess generalization capabilities from a comprehensive clinical perspective, the final architecture was evaluated on the independent test set across two scales: window and EGM levels (via majority voting of individual activation windows). As detailed in , the model demonstrated robust quantitative performance for fibrotic substrate identification, achieving a window-level AUPR of 0.943 (c) and an EGM-level Dice score of 0.866. Beyond these standard metrics, mapping the EGM-level predictions back onto the 3D atrial geometries (b) confirmed a close anatomical accuracy with the ground-truth (Figure a); the predicted maps successfully delineated the irregular fibrotic patches without generating excessive false positives in healthy anatomical regions.

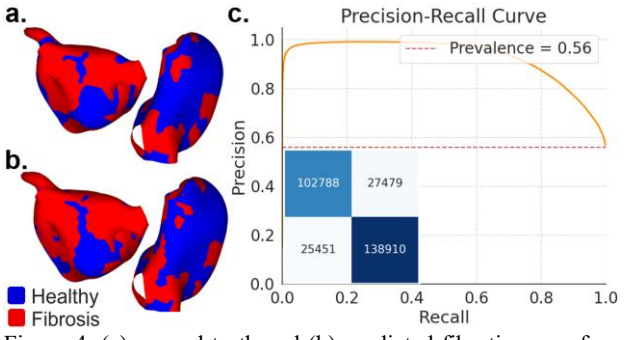

Figure 4. (a) ground-truth and (b) predicted fibrotic maps from atrial geometry (test); and (c) displays the global Precision-Recall curve alongside the window-level results and confusion matrix at the optimal classification threshold.

Table 2. Test set performance metrics.

Eval. Approach	AUPR	Precision	Recall	Dice
Window-level	0.943	0.892	0.836	0.862
EGM-level		0.903	0.832	0.866

4. Discussion and conclusions

In this study, we developed a 1D-CNN to identify atrial fibrosis from isolated EGMs using simulated bi-atrial anatomies. Our findings demonstrated that bipolar electrograms, minimal electrode-to-endocardium distances, and highly localized labeling radii better correlated with fibrotic substrate presence. The final model exhibited robust predictive performance across window and EGM levels, successfully delineating complex fibrotic patches with high anatomical accuracy (Dice of 0.866) when mapped onto 3D geometries.

These optimal configurations align with established biophysical principles and clinical practice. Bipolar EGMs outperformed unipolar signals due to their higher spatial resolution, effectively capturing local electrical activity while rejecting far-field influence (i.e., remote atrial activation in this case), as has been seen in the literature [10]. Furthermore, while minimal recording distances more accurately emulate the contact between the electrode and the endocardial wall, small labeling radii confirm that fibrosis-induced EGM abnormality is a highly localized phenomenon [4].

Our predictive capabilities notably competitive with recent computational approaches [2–4]. While these studies successfully identified fibrotic regions using handcrafted signal features [2] or advanced mathematical indices [3, 4], they were developed on simplified 2D simulations. In contrast, our approach eliminates the need for prior feature extraction by processing raw standard EGMs, demonstrating robust anatomical delineation across complex 3D bi-atrial anatomies.

Despite these promising results, the model was trained exclusively on synthetic data from a limited number of simulations. Furthermore, binarization resulted in a loss of spatial resolution in fibrotic patches. Future work must incorporate crucial factors to ensure overall algorithmic robustness and clinical translation, including ventricular far-field activity, adipose tissue infiltrations, diverse electrode types, clinical recordings and a multi-class approach.

In conclusion, this proof-of-concept study demonstrates that simplified 1D-CNNs can effectively extract morphological features from EGMs for accurate fibrotic substrate identification. With further clinical validation, this computational pipeline has the potential to characterize the arrhythmogenic substrate with the aim of optimizing therapeutic planning and guiding personalized ablation strategies.

Acknowledgments

This work was funded by Generalitat Valenciana Grant CIAICO/2024/247, and PID2023-148702OB-I00 and EraNet PCI2024-153442 funded by MCIN/ 10.13039/501100011033 and by "ERDF A way of making Europe".

References

[1] G. Lippi *et al.*, "Global epidemiology of atrial fibrillation: An increasing epidemic and public health challenge," *Int. J. Stroke*, vol. 16, no. 2, pp. 217-221, 2021.

[2] J. Sánchez *et al.*, "Using machine learning to characterize atrial fibrotic substrate from intracardiac signals with a hybrid in silico and in vivo dataset," *Front. Physiol.*, vol. 12, 2021.

[3] J. Riccio *et al.*, "Omnipolar EGM voltage mapping for atrial fibrosis identification evaluated with an electrophysiological model," in *28th Eur. Signal Process. Conf. (EUSIPCO)*, pp. 920-924, 2021.

[4] J. Riccio *et al.*, "Atrial fibrosis identification with unipolar electrogram eigenvalue distribution analysis in multi-electrode arrays," *Med. Biol. Eng. Comput.*, vol. 60, no. 11, pp. 3091-3112, 2022.

[5] J. T. Koivumäki *et al.*, "Impact of sarcoplasmic reticulum calcium release on calcium dynamics and action potential morphology in human atrial myocytes: A computational study," *PLoS Comput. Biol.*, vol. 7, no. 1, 2011.

[6] G. S. Romitti *et al.*, "Virtual population-based analysis of anatomical and electrophysiological risk markers for atrial fibrillation," *JRSM Cardiovasc. Dis.*, vol. 15, 2026.

[7] V. Garcia-Molla *et al.*, "Adaptive step ode algorithms for the 3d simulation of electric heart activity with graphics processing units," *Comput. Biol. Med.*, vol. 44, pp. 15-26, 2014.

[8] G. S. Romitti, M. Termenón-Rivas, A. Liberos, and M. Rodrigo, "Modeling fibrosis infiltration in a virtual cohort: Impact on atrial fibrillation vulnerability," *Comput. Cardiol.*, 2025.

[9] M. Rodrigo *et al.*, "Impact of catheter configuration on the mapping of atrial fibrillation," *Circ. Arrhythm. Electrophysiol.*, vol. 19, no. 3, 2026.

[10] D. Nairn *et al.*, "Comparison of Unipolar and Bipolar Voltage Mapping for Localization of Left Atrial Arrhythmogenic Substrate in Patients With Atrial Fibrillation," *Front. Physiol.*, vol. 11, 2020.

Address for correspondence:

Miguel Rodrigo
Av. de la Universidad s/n, 46100, Burjassot, Valencia, Spain.
miguel.rodrigo@uv.es.